High-pressure study of methyl formate oxidation and its interaction with NO

*Lorena Marrodán, Ángela Millera, Rafael Bilbao, María U. Alzueta**

Aragón Institute of Engineering Research (I3A). Department of Chemical and Environmental Engineering. University of Zaragoza. C/ Mariano Esquillor, s/n. 50018 Zaragoza. Spain

*Phone: +34976761876/Fax: +34976761879, e-mail: uxue@unizar.es

ABSTRACT

An experimental and modeling study of the influence of pressure on the oxidation of methyl formate (MF) has been performed in the 1-60 bar pressure range, in an isothermal tubular quartz flow reactor in the 573-1073 K temperature range. The influence of stoichiometry, temperature, pressure and presence of NO on the conversion of MF and on the formation of the main products (CH_2O, CO_2, CO, CH_4 and H_2) has been analyzed. A detailed kinetic mechanism has been used to interpret the experimental results. The results show that the oxidation regime of MF differs significantly from atmospheric to high pressure conditions. The impact of the NO presence has been considered, and results indicate that no net reduction of NO_x is achieved, even though at high pressure, the NO-NO_2 inter-conversion results in a slightly increased reactivity of MF.

KEYWORDS: methyl formate, high-pressure, oxidation, nitric oxide, kinetic model.

Introduction

Nowadays, there is an increasing urgency in finding ways to improve fuel economy of motor vehicles while controlling exhaust emissions to meet ever-tighter emission regulations. Diesel engines exhibit a better fuel economy and lower emissions of unburned hydrocarbons and CO, compared to gasoline fueled engines. However, they suffer from high emissions of particulate matter and NO_x, which are hard to reduce simultaneously.

Methods to reduce both emissions include high-pressure injection, turbocharging and the use of fuel additives; the latest is thought to be one attractive and effective solution [1]. Dimethylether (DME) and dimethoxymethane (DMM) are two examples of promising additives for diesel fuel and/or substitutes [2-6]. Methyl formate (MF, CH_3OCHO) has been found to be a byproduct of the oxidation of several proposed fuel alternatives, such as these two, DME [7-9] and DMM [10, 11]. MF is the simplest ester, and esters are the primary constituents of biodiesel [12, 13]. MF has also been considered as a model molecule used to understand biodiesel and other such real fuel molecules combustion [14, 15].

Esters are volatile organic compounds and may be released into the atmosphere during their employment (e.g. manufacture of perfumes and food flavoring, industrial solvents, fuel burning) or from natural sources (i.e., vegetation). Methyl formate has been reported to be active as well in the atmosphere and while many studies have been reported in the literature on the conversion of MF in the atmosphere [e.g., 16], few studies addressing the conversion of MF at high temperatures, from both experimental and kinetic modeling points of view, have been reported [12, 14-15, 17-22] and even less in terms of high-pressure. Francisco [21] suggested a mechanism for CH_3OCHO decomposition with two parallel reactions forming $CH_3OH + CO$ and $CH_2O + CH_2O$, and later Dooley et al. [12] found that the rate constant value for MF decomposition proposed by Francisco [21] was not consistent with their

experimental results. Metcalfe et al. [15] computed pressure-dependent rate constants for MF decomposition with ab initio methods and confirmed that computations of Francisco might be in error. The MF decomposition seems to be dominated by a single channel producing methanol and carbon monoxide over all temperatures and pressures. Other two possible channels (producing two molecules of formaldehyde, and $CH_4 + CO_2$) appear to be of minor relevance.

Among all the previous studies reported, it is worthwhile to mention an earlier work of our research group (Alzueta et al. [17]) on MF conversion at atmospheric pressure, which has been taken as starting point of the present work. The earlier study was carried out in an experimental setup that operates at atmospheric pressure in the 300-1000 K temperature range and for different stoichiometries (λ=0, 0.7, 1 and 35). That work suggests $CH_3OCHO \rightarrow CH_3OH \rightarrow CH_2OH/CH_3O \rightarrow CH_2O \rightarrow HCO \rightarrow CO \rightarrow CO_2$ as main reaction pathway, and the $HCOOCH_3$ (+M)$\rightleftharpoons CH_3OH+CO$ (+M) reaction was found to play an important role in MF conversion. That work also analyzed the influence of the presence of NO on MF conversion at atmospheric pressure, and it was found that the addition of NO does not produce any variation of the MF conversion regime, except for oxidizing conditions when MF conversion is shifted to lower temperatures, due to the fact that a route producing CH_2OCHO radicals becomes more active, compared to the above mentioned reaction pathway. Nevertheless, the consumption of MF does not result in net decrease of NO_x.

In this context, the present work aims to extend the experimental database of flow reactor data on MF oxidation to different pressures (above atmospheric pressure), since these results will be helpful for engine developments. Because of the fact that NO can be produced in the combustion chamber of the engine, the interaction between MF and NO is also analyzed by adding a given amount of NO (at a constant pressure, 20 bar). The NO evolution at high-

pressure in the NO_x interaction with $CO/H_2/O_2$ has been previously studied by Rasmussen et al. [23] and in the C_2H_4/NO_x interaction by Giménez-López et al. [24].

Specifically, the oxidation of MF has been investigated under flow reactor conditions, in a new high pressure setup, at different pressures (atmospheric, 20, 40 and 60 bar), in the 573-1073 K temperature interval, from reducing to very fuel-lean conditions, both in the absence and in the presence of NO. Additionally, the experimental data are interpreted in terms of a detailed kinetic modeling study based on the MF mechanism subset by Dooley et al. [12], updated by Alzueta et al. [17] and revised and completed in the present work.

Experimental

Oxidation experiments of MF (both in the presence and in the absence of NO) were carried out in an experimental installation (Fig. 1), which consists of a feeding system (gas/liquid), a reaction system and a gas analysis system.

This installation is provided with a CEM (Controlled Evaporation Mixer), which evaporates liquids and mix them with a carrier gas. MF liquid is supplied from a pressurized tank through a liquid mass flow controller (MFM) and evaporated in the CEM using N_2 as carrier gas. A concentration of approximately 3000 ppm of MF is introduced in all experiments with an uncertainty of the measurements below 10%. Due to the fact that the feeding is a liquid, some punctual fluctuations may occur during the experiments.

All gases are supplied from gas cylinders through gas mass flow controllers (MFC). The amount of O_2 used depends on the air excess ratio (λ), defined as the inlet oxygen concentration divided by stoichiometric oxygen. A concentration of approximately 3000 ppm of NO has been used in the experiments conducted with NO. The 3000 ppm NO concentration

value was chosen to be of a similar order of magnitude as the MF feed (i.e. 6000 ppm of C), with a NO/C ratio of 1/2, which falls within the 1/12 to 1 NO/C range of previous studies of our research group [25].

Nitrogen is used to balance, resulting in a constant flow rate of 1000 mL(STP)/min. All the experimental mixtures are diluted in nitrogen. Therefore, little heat is released during the reaction, and isothermal conditions can be considered.

The reaction system consists of a quartz reactor (i.d. 6 mm, 1500 mm in length), enclosed in a stainless steel tube that acts as a pressure shell. A pressure control system, consisting of two thermal mass flow pressure controllers (MFPC), automatically delivers N_2 to the shell-side of the reactor to obtain a pressure similar to that inside the reactor, avoiding the reactor breaking. Pressure inside the reaction chamber is controlled within ±1%. The steel tube is placed horizontally in a tubular oven, with three individually controlled electrical heating elements, that ensure an isothermal reaction zone of approximately 56 cm with a uniform temperature profile (±10 K). The reactor temperature is monitored by type K thermocouples positioned between the quartz reactor and the steel shell. An example of temperature profiles inside the reactor can be found as supplementary material.

The gas residence time, t_r, in the isothermal zone depends on the reaction temperature and pressure, $t_r(s)=261.1*P(bar)/T(K)$. The experiments were carried out at different pressures (atmospheric, 20, 40 and 60 bar) and in the 573-1073 K temperature range. Table 1 lists the conditions of the experiments.

All the reactants (gases and the evaporated liquid) are premixed before entering the reactor and pressurized from gas cylinders. The reactor pressure is monitored upstream the reactor by a differential pressure transducer and controlled by a pneumatic pressure valve positioned after the reactor, which can operate at pressures up to 80 bar. Downstream the reactor, the

pressure is reduced to atmospheric level. Previous to the gas analysis, gases pass through a filter and a condenser to assure gas cleaning and water-free content which could affect the analysis equipment.

Products are analyzed by a gas chromatograph equipped with TCD detectors, able to detect MF, CO, CO_2, H_2, CH_3OH, CH_2O and hydrocarbons (CH_4, C_2H_2, C_2H_4 C_2H_6); a continuous IR analyzer to measure the NO concentration; and a Fourier Transform Infrared (FTIR) spectrometer to check the formation of some nitrogen compounds such as NO_2, HCN or NH_3. The uncertainty of measurements is estimated as ±5%, except for the FTIR spectrometer, which is estimated as ±10%.

In order to evaluate the goodness of the experiments, the atomic carbon balance was checked in all experiments, and resulted to close always better than 94%.

Reaction chemical kinetic mechanism

The present experimental results have been analyzed in terms of a detailed chemical kinetic model for the oxidation of MF in the absence and presence of NO at different pressures. The full mechanism takes as starting point an earlier work on MF conversion at atmospheric pressure [17] which includes the Dooley et al. MF reaction subset [18], even though it has been revised according to the present high pressure conditions and the presence of NO taking into account the considerations of Rasmussen et al. [23, 26-27] and Giménez-López et al. [24].

The decomposition reaction of MF, with CH_3OH and CO as main products, constitutes the beginning of the MF oxidation. The methanol formed is rapidly consumed giving mainly hydroxymethyl radicals and these, formaldehyde. Under oxidizing conditions, MF also

produces CH_2OCHO and CH_3OCO radicals by hydrogen abstraction reactions. All these reactions will be discussed in depth later through the reaction path diagram for MF oxidation.

In particular, results appeared to be sensitive to the HO_2CH_2OCHO species, involved in the formation of CO_2 ($HO_2CH_2OCHO \rightarrow OCH_2OCHO \rightarrow HCOO \rightarrow CO_2$). Therefore, in order to represent the experimental results by the model, reactions concerning HCOO and HCOOH had to be added to the mechanism. For the $HCOOH+OH \rightleftharpoons HCOO+H_2O$ reaction, we have adopted the theoretically determined values of kinetic parameters by Galano et al. [28], and for $HCOO \rightleftharpoons H+CO_2$, the determination of Larson et al. [29] was used.

Under the present combustion conditions and without NO, the main reaction products are formaldehyde, CO, CO_2, CH_4 and H_2. In the presence of NO in the reactant mixture, it has been observed that when the pressure is increased from atmospheric to 20 bar, NO is converted almost completely to NO_2, as has been reported in previous works [24, 26]. The main reaction involved in this conversion is $NO+NO+O_2 \rightleftharpoons NO_2+NO_2$, which gains relevance with the pressure. This reaction has already been studied [30-32], but the pressure dependence of the kinetic parameters is not well known presently, and the uncertainty related to it may be significant. For this reaction, we have adopted the value determined by Park et al. [32], which was also selected in the high pressure work of Rasmussen et al. [26].

Model calculations have been performed using Senkin, the plug flow reactor code that runs in conjunction with the Chemkin-II library [33, 34], considering pressure and temperature constant in the reaction zone, which has been tested to be a fairly good assumption. The full mechanism listing and thermochemistry used can be found as supplementary material.

Results and discussion

In this work, a study of the oxidation of MF at different pressures (1, 20, 40, and 60 bar) and in the 573-1073 K temperature interval has been carried out. In addition to temperature and pressure, the influence of stoichiometry (λ=0.7, 1 and 20) and the presence of NO (approximately 3000 ppm) on oxidation process have been also analyzed.

Oxidation of MF in the absence of NO.

Figure 2 shows the influence of temperature and stoichiometry at a given pressure (20 bar) on the concentration of MF and the formation of the main products of the reaction: CH_2O, CO_2, CO, CH_4 and H_2. The concentration values are shown as function of temperature for three different stoichiometries, λ=0.7, 1 and 20. Figure 2 compares experimental (symbols) and simulation (lines) results. The model predicts the general trend of the different concentration profiles, but there are some discrepancies between experimental and simulation results. These discrepancies, especially in the profiles of CO_2, may be attributed to the small fluctuations in the liquid flow fed using the CEM previously mentioned, and/or to the uncertainty in model calculations.

The temperature for the onset of the MF oxidation is approximately 723 K according to the experimental results, independently on the stoichiometry, with MF almost converted at 873 K in all the cases. This onset temperature is lower than that needed in the case of MF oxidation at atmospheric pressure [17].

The oxygen concentration in the reactant mixture slightly influences the conversion of MF, similarly to what has been observed in the oxidation behavior of other oxygenated compounds, such as DME [35]. However, the presence of oxygen does have certain effects on some of the reaction products. The conversion of MF is accompanied by the formation of both

CO and CO_2, which are the main products in all the experiments performed. At higher temperatures, when CO has reached its maximum concentration and it begins to drop, CO_2 increases its concentration up to an almost constant value, which is reached at lower temperatures for smaller values of lambda.

Under oxidizing conditions, the formation of CO_2 is favored and, consequently, a lower amount of CO is produced, whereas other products such as CH_4 or H_2 are hardly formed.

Figure 3 shows a reaction path diagram for MF oxidation obtained through a reaction rate analysis with the mechanism compiled in the present work. For the conditions of Figure 2, the MF oxidation is initiated by the following decomposition reaction, which is in agreement with other previous works [10, 15],

$CH_3OCHO\ (+M) \rightleftharpoons CH_3OH + CO\ (+M)$ (r.1),

with minor relevance of:

$CH_3OCHO\ (+M) \rightleftharpoons CH_4 + CO_2\ (+M)$ (r.2), and

$CH_3OCHO\ (+M) \rightleftharpoons CH_2O + CH_2O\ (+M)$ (r.3).

Both products, CH_4 and CH_2O, are detected as final products in the reaction process.

The methanol produced by reaction r.1 is consumed by a number of reactions (r.4-r.6) giving mainly hydroxymethyl radicals:

$CH_3OH + OH \rightleftharpoons CH_2OH + H_2O$ (r.4)

$CH_3OH + H \rightleftharpoons CH_2OH + H_2$ (r.5)

$CH_3OH + HO_2 \rightleftharpoons CH_2OH + H_2O_2$ (r.6),

which react mainly with molecular oxygen to give formaldehyde:

$CH_2OH + O_2 \rightleftharpoons CH_2O + HO_2$ (r.7).

When formaldehyde has been produced, it continues the $CH_2O \rightarrow HCO \rightarrow CO \rightarrow CO_2$ reaction sequence.

Under oxidizing conditions, calculations indicate that MF also produces CH_2OCHO and CH_3OCO radicals by hydrogen abstraction reactions, as reported in previous studies [36, 37], i.e.:

$CH_3OCHO + OH \rightleftharpoons CH_2OCHO + H_2O$ (r.8)

$CH_3OCHO + OH \rightleftharpoons CH_3OCO + H_2O$ (r.9).

For example, at 1 bar and stoichiometric conditions (λ=1), reaction r.1 (CH_3OCHO (+M)$\rightleftharpoons CH_3OH + CO$ (+M)) is the dominant reaction pathway with a relative importance of 86%, whereas, at 20 bar and oxidizing conditions (λ=20), the reaction r.8 has a relative importance of approximately 62% and reaction r.9, of 20%.

At low residence times (i.e. around 0.3 s, at 1 bar), CH_2OCHO is found, in part, to decompose thermally to give formaldehyde and formyl radical through reaction r.10; but, at higher residence times (i.e. around 6-8 s, at 20 bar), it mostly follows the path represented by the reactions r.11-r.13.

$CH_2OCHO \rightleftharpoons CH_2O + HCO$ (r.10)

$CH_2OCHO + HO_2 \rightleftharpoons HO_2CH_2OCHO$ (r.11)

$HO_2CH_2OCHO \rightleftharpoons OCH_2OCHO + OH$ (r.12)

$OCH_2OCHO \rightleftharpoons CH_2O + HCOO$ (r.13).

The hydrocarboxyl radical decomposes:

$HCOO \rightleftharpoons H + CO_2$ (r.14).

The CH_3OCO radical formed in the reaction r.9 decomposes thermally to give CO_2 as final product, and methyl radicals,

$CH_3OCO \rightleftharpoons CH_3 + CO_2$ (r.15).

Under the high-pressure conditions of this work, the stable methyl radical can generate methane. Which is found as final reaction product, but can also form methoxy radicals through reaction r.16, which further decomposes giving formaldehyde (r.17) that can go through the already mentioned reaction sequence to give CO_2 as final product.

$CH_3 + HO_2 \rightleftharpoons CH_3O + OH$ (r.16)

$CH_3O\ (+M) \rightleftharpoons H + CH_2O\ (+M)$ (r.17).

Methanol also forms methoxy radicals by hydrogen abstraction reactions with OH and H radicals in oxidizing conditions,

$CH_3OH + OH \rightleftharpoons CH_3O + H_2O$ (r.18)

$CH_3OH + H \rightleftharpoons CH_3O + H_2$ (r.19).

For the highest value of lambda studied (λ=20), the CH_4 produced is lower as seen in Figure 2. This is attributed to the fact that reaction r.16 is favored under oxidative conditions. In the case of stoichiometric or reducing conditions and for the high pressures of this work, other reactions of CH_3 (with MF) start to become more important and produce CH_4 as product:

$CH_3 + CH_3OCHO \rightleftharpoons CH_2OCHO + CH_4$ (r.20)

$CH_3 + CH_3OCHO \rightleftharpoons CH_3OCO + CH_4$ (r.21).

A first-order sensitivity analysis for CO has been performed for all the sets in Table 1. The results obtained are shown in Table 2. The data of Table 2 indicate that the conversion of MF is mostly sensitive to the unimolecular decomposition of MF to give methanol and carbon monoxide (r.1). Reactions giving CH_2OCHO and CH_3OCO radicals appear also to be sensitive, especially in presence of NO and for the highest value of lambda studied (λ=20).

A study of the influence of varying pressure on MF oxidation has also been performed. Experiments at different pressures, from atmospheric to 60 bar, and for stoichiometric conditions have been carried out (Table 1). The results obtained are shown in Figure 4.

As can be seen, there is a huge difference between the results at atmospheric pressure and higher ones. At 1 bar, the temperature for the onset of the conversion of MF is near 873 K and it is clearly higher than the required for 20 bar, 723 K. However, the effect of increasing pressure between 20 and 60 bar is seen to be less pronounced compared to the changes found from 1 to 20 bar. For example, as can be seen in Figure 4, the maximum concentration of CH_4 for atmospheric pressure is reached at approximately 973 K; for 20 and 40 bar, at 798 K; and finally for the highest value of pressure (60 bar), at 748 K. Increasing pressure above atmospheric conditions shifts the concentration profiles to almost approximately 200 K less.

Results indicate that at the highest pressure studied (60 bar), the formation of CO_2 is favored and, therefore, a smaller amount of CO is produced. In the cases of 20 and 40 bar, the amounts of CO and CH_4 produced experimentally are almost similar, and higher than those predicted by the model. Calculations match reasonably well with the experimental trends; the biggest discrepancy is found in the CO_2 concentration profile.

Under atmospheric pressure conditions, MF decomposes giving CH_3OH via reaction r.1 and with minor relevance via reactions r.2 and r.3 [17]. When the pressure is raised, the reaction pathways become slightly more complex. At 20 bar, the MF oxidation is also initiated by its

decomposition into CH_3OH and CO (r.1), but as the pressure increases, all the reactions become faster and reactions of MF with OH radicals (r.8 and r.9) become more relevant (i.e. at 60 bar, 51% and 16% of relative importance, respectively, for reactions r.8 and r.9), producing CH_2OCHO and CH_3OCO radicals. The CH_2OCHO radical reacts, in presence of MF, to produce the CH_3OCO radical, and also reacts with HO_2 by reaction r.11 and following the r.12-r.14 reaction sequence until CO_2 is generated. The CH_3OCO radical decomposes thermally producing CO_2 and methyl radicals (r.15).

All these reaction sequences are responsible for the formation of CO_2, favored at high pressures, and it is found to occur at lower temperatures compared to the low pressure conditions.

Oxidation of MF in the presence of NO.

The influence of the NO presence on MF oxidation has been considered for different stoichiometries at a given pressure of 20 bar. Figure 5 shows the results obtained of MF conversion, and the formation of CO and CO_2. It is worthwhile to note that the presence of NO in the reactant mixture has its main effect on the decrease of other final products different from CO_2 or CO, since CH_4 or CH_2O are not formed in appreciable amounts. Besides, the MF presents a slightly increased reactivity.

Figure 5 also shows the results of NO obtained under the conditions studied. For the high pressure considered (20 bar), principally for the lowest studied temperatures, the concentration of NO at the outlet of the reaction system is very low, and it is attributed to the fact that the conversion of NO to NO_2 is clearly favored. This is attributed to the fact that most of NO is converted to NO_2 when the pressure is raised above atmospheric, through:

$NO + NO + O_2 \rightleftharpoons NO_2 + NO_2$ (r.22),

And through the important equilibrium between NO and NO_2,

$NO + HO_2 \rightleftharpoons NO_2 + OH$ (r.23),

which is relevant under high pressure conditions [24]. However, results indicate no net reduction of NO_x in the studied conditions.

Model calculations indicate that the reaction pathways change with the presence of NO and/or the NO_2 formed. Figure 6 shows a reaction path diagram for MF oxidation in the presence of NO obtained in a similar manner to Figure 3, i.e., through a reaction rate analysis with the mechanism compiled in the present work. Although the MF oxidation starts also by reaction r.1, CH_2OCHO and CH_3OCO radicals are highly formed under the studied conditions. The CH_2OCHO radical, with MF, reacts giving other radical, CH_3OCO, as product. It decomposes thermally through reaction r.15, and subsequently the CH_3 formed reacts with NO_2 giving nitromethane:

$CH_3 + NO_2 \rightleftharpoons CH_3NO_2$ (r.24).

CH_3NO_2 continues the $CH_3NO_2 \rightarrow CH_2NO_2 \rightarrow CH_2O$ reaction sequence, and formaldehyde also reacts with NO_2:

$CH_2O + NO_2 \rightleftharpoons HONO + HCO$ (r.25)

$HONO \rightleftharpoons NO + OH$ (r.26).

The HCO produced can react either with molecular oxygen or with NO_2,

$HCO + O_2 \rightleftharpoons HO_2 + CO$ (r.27)

$HCO + NO_2 \rightleftharpoons NO + CO_2 + H$ (r.28),

which contributes to the NO_2-NO interconversion.

The last two reactions are in competition at stoichiometric and reducing conditions, but under oxidizing conditions reaction with oxygen (r.27) becomes dominant.

For the most oxidizing conditions considered, i.e. λ=20, the reaction pathways mentioned change slightly. With an excess of O_2, the radical CH_2OCHO follows another reaction sequence, through some intermediate oxygenated compounds, i.e. $CH_2OCHO \rightarrow OOCH_2OCHO \rightarrow HOOCH_2OCHO \rightarrow OCH_2O_2H \rightarrow CH_2O$, to give formaldehyde as product, which reacts with NO_2 as mentioned above (r.25). In the presence of NO_2, CO can also react producing CO_2 and NO,

$$CO + NO_2 \rightleftharpoons NO + CO_2 \qquad \text{(r.29)},$$

with no net NO_x reduction, as has been mentioned.

Conclusions

The oxidation of MF has been studied in a tubular quartz flow reactor in the 573-1073 K temperature interval, for different stoichiometries (λ=0.7, 1 and 20) and also different pressures, from atmospheric conditions to 60 bar. The experimental data obtained have been interpreted in terms of a detailed chemical kinetic mechanism, taken from literature and updated and revised in the present work.

The stoichiometry has been found to have certain effects on the main products of the oxidation of MF. Under oxidizing conditions, the formation of CO_2 is favored, and thus a lower amount of CO is produced, whereas other products (CH_4 or H_2) are hardly formed. MF conversion is clearly shifted toward lower temperatures, around 200 K, when the pressure is increased from 1 to 20 bar and over.

The reaction pathways occurring at high pressure are a bit more complex than those observed at atmospheric conditions, due to the formation of CH_2OCHO and CH_3OCO radicals, which are not so relevant at atmospheric pressure.

The addition of NO to the reactant mixture has its main effect on the decrease of other final products different from CO_2 or CO. When pressure is raised above atmospheric, most of the NO is converted to NO_2, which exhibits a high reactivity, taking part in many reactions with the intermediates formed. However, results indicate that no net reduction of NO_x is achieved in the MF-NO interaction at high pressure.

Acknowledgements

The authors express their gratitude to the Aragón Government (GPT group) and to MINECO and FEDER (Project CTQ2012-34423), for financial support. Authors also would like to acknowledge to the "*Servicio General de Apoyo a la Investigación-SAI"* of the University of Zaragoza for its contribution to the build-up of the experimental setup.

Supporting Information

Information on temperature profiles inside the reactor, the full mechanism listing and the thermochemistry used. This material is available free of charge via the Internet at http://pubs.acs.org.

References

[1] Yanfeng, G.; Shenghua, L.; Hejun, G.; Tiegang, H.; Longbao, Z. *Appl. Therm. Eng*. 2007, 27, 202-207.

[2] Sorenson, S.C.J. *J. Eng. Gas Turbines Power* 2001, 123, 652-658.

[3] Song, R.; Li, K.; Feng, Y.; Liu, S. *Energy Fuels* 2009, 23, 5460-5466.

[4] Esarte, C.; Millera, A.; Bilbao, R.; Alzueta, M.U. *Ind. Eng. Chem. Res*. 2010, 49, 6772-6779.

[5] Song, K.H.; Litzinger, T.A. *Combust. Sci. Technol*. 2006, 178, 2249-2280.

[6] Sathiyagnanam, A.P.; Saravanan, C.G. *Fuel* 2008, 87, 2281-2285.

[7] Gao, J.; Nakamura, Y. *Fuel* 2013, 106, 241-248.

[8] Herrmann, F.; Jochim, B.; Oßwald, P.; Cai, L.; Pitsch, H.; Kohse-Höinghaus, K. *Combust. Flame* 2014, 161, 384-397.

[9] Herrmann, F.; Oßwald, P.; Kohse-Höinghaus, K. *Proc. Combust. Inst.* 2014, 34, 771-778.

[10] Daly, C.A.; Simmie, J.M.; Dagaut, P.; Cathonnet, M. *Combust. Flame* 2001, 125, 1106-1117.

[11] Chen, G.; Yu, W.; Fu, J.; Mo, J.; Huang, Z.; Yang, J.; Wang, Z.; Jin, H., Qi, F. *Combust. Flame* 2012, 159, 2324-2335.

[12] Dooley, S.; Dryer, F.L.; Yang, B.; Wang, J.; Cool, T.A.; Kasper, T.; Hansen, N. *Combust. Flame* 2011, 158, 732-741.

[13] Pitz, W.J.; Mueller, C. J. *Prog. Energy Combust. Sci.* 2011, 37, 330-350.

[14] Ren, W.; Lam, K.-Y.; Pyun, S.H.; Farooq, A.; Davidson, D.F.; Hanson, R.K. *Proc. Combust. Inst.* 2014, 34, 453-461.

[15] Metcalfe, W.K.; Simmie, J.M.; Curran, H.J. *J. Phys. Chem. A* 2010, 114, 5478-5484.

[16] Wallington, T.J.; Hurley, M.D.; Maurer, T.; Barnes, I.; Becker, K.H.; Tyndall, G.S.; Orlando, J.J.; Pimentel, A.S.; Bilde, M. *J. Phys. Chem. A* 2001, 105, 5146-5154.

[17] Alzueta, M.U.; Aranda, V.; Monge, F.; Millera, A.; Bilbao, R. *Combust. Flame* 2013, 160, 853-860.

[18] Dooley, S.; Burke, M.P; Chaos, M.; Stein, Y.; Dryer, F.L.; Zhukov, V.P.; Finch, O.; Simmie, J.M.; Curran, H.J. *Int. J. Chem. Kinet*. 2010, 42, 527-549.

[19] Good, D.A.; Hanson, J.; Francisco, J.S.; Li, Z.; Jeong, G.R. *J. Phys. Chem. A* 1999, 103, 10893-10898.

[20] Good, D.A.; Francisco, J.S. *J. Phys. Chem. A* 2000, 104, 1171-1185.

[21] Francisco, J.S. *J. Am. Chem. Soc*. 2003, 125, 10475-10480.

[22] Westbrook, C.K.; Pitz, W.J.; Westmoreland, P.R.; Dryer, F.L.; Chaos, M.; Osswald, P.; Kohse-Höinghaus, K.; Cool, T.A.; Wang, J.; Yang, B.; Hansen, N.; Kasper, T. *Proc. Combust. Inst.* 2009, 32, 221-228.

[23] Rasmussen, C.L.; Jakobsen, J.G.; Glarborg, P. *Int. J. Chem. Kinet*. 2008, 40, 778-807.

[24] Giménez-López, J.; Alzueta, M.U.; Rasmussen, C.L.; Marshall, P.; Glarborg, P. *Proc. Combust. Inst.* 2011, 33, 449-457.

[25] Abián, M; Silva, S.L.; Millera, A.; Bilbao, R.; Alzueta, M.U. *Fuel Process. Technol*. 2010, 91, 1204-1211.

[26] Rasmussen, C.L.; Hansen, J.; Marshall, P.; Glarborg, P. *Int. J. Chem. Kinet*. 2008, 40, 454-480.

[27] Rasmussen, C.L.; Rasmussen, A.E.; Glarborg, P. *Combust. Flame* 2008, 154, 529-545.

[28] Galano, A.; Álvarez-Idaboy, J.R.; Ruiz-Santoyo, M.E.; Vivier-Bunge, A. *J. Phys. Chem. A* 2002, 106, 9520-9528.

[29] Larson, C.W.; Steward, P.H.; Golden, D.M. *Int. J. Chem. Kinet*. 1998, 20, 27-40.

[30] Olbregts, J. *Int. J. Chem. Kinet*. 1985, 17, 835-848.

[31] Röhring, M.; Petersen, E.L.; Davidson, D.F.; Hanson, R.K. *Int. J. Chem. Kinet*. 1997, 29, 483-494.

[32] Park, J.; Giles, N.D.; Moore, J.; Lin, M.C. *J. Phys. Chem. A* 1998, 102, 10099-10105.

[33] Lutz, A.E.; Kee, R.J.; Miller, J.A. Senkin: A Fortran Program for Predicting Homogeneous Gas Phase Chemical Kinetics with Sensitivity Analysis, Sandia National Laboratories, Report SAND87-8248, 1988.

[34] Kee, R.J.; Rupley, F.M.; Miller, J.A. Chemkin-II: A Fortran Chemical Kinetics Package for the Analysis of Gas-Phase Chemical Kinetics, Sandia National Laboratories, Report SAND87-8215, 1991.

[35] Alzueta, M.U.; Muro, J.; Bilbao, R.; Glarborg, P. *Isr. J. Chem*. 1999, 39, 73-86.

[36] Tan, T.; Pavone, M.; Krisiloff, D.B.; Carter, E.A. *J. Phys. Chem. A* 2012, 116, 8431-8443.

[37] Lam, K-Y.; Davidson, D.F.; Hanson, R. K. *J. Phys. Chem. A* 2012, 116, 12229-12241.

Table captions

Table 1. Matrix of experimental conditions. The experiments are conducted at constant flow rate of 1000 mL(STP)/min, in the temperature interval of 573-1073 K. The balance is closed with N_2. The residence time depends on the reaction temperature and pressure: t_r(s)=261.1*P(bar)/T(K).

Table 2. Linear sensitivity coefficients for CO for Sets 1-9. (The sensitivity coefficients are given as $A_i\delta Y_j/Y_j\delta A_i$, where A_i is the pre-exponential constant for reaction i and Y_j is the mass fraction of j_{th} species. Therefore, the sensitivity coefficients listed can be interpreted as the relative change in predicted concentration for the species j caused by increasing the rate constant for reaction i by a factor of 2).

Tables

Table 1
Matrix of experimental conditions. The experiments are conducted at constant flow rate of 1000 mL(STP)/min, in the temperature interval of 573-1073 K. The balance is closed with N_2. The residence time depends on the reaction temperature and pressure: $t_r(s)=261.1*P(bar)/T(K)$.

Exp.	MF (ppm)	O_2 (ppm)	NO (ppm)	λ	P (bar)
Set 1	3056	4200	0	0.7	20
Set 2	2794	6000	0	1	20
Set 3	2547	120000	0	20	20
Set 4	3166	6000	0	1	1
Set 5	2489	6000	0	1	40
Set 6	2238	6000	0	1	60
Set 7	2375	4200	3020	0.7	20
Set 8	2400	6000	2745	1	20
Set 9	2209	120000	3000	20	20

Table 2
Linear sensitivity coefficients for CO for Sets 1-9. (The sensitivity coefficients are given as $A_i\delta Y_j/Y_j\delta A_i$, where A_i is the pre-exponential constant for reaction i and Y_j is the mass fraction of j_{th} species. Therefore, the sensitivity coefficients listed can be interpreted as the relative change in predicted concentration for the species j caused by increasing the rate constant for reaction i by a factor of 2).

Reaction	Set 1 (723K)	Set 2 (723K)	Set 3 (698K)	Set 4 (823K)	Set 5 (673K)	Set 6 (673K)	Set 7 (748K)	Set 8 (748K)	Set 9 (698 K)
$CH_3OCHO(+M)=CH_3OH+CO(+M)$	0.396	0.287	0.024	0.982	0.018	0.000	0.943	0.940	0.813
$CH_3OCHO+OH=CH_2OCHO+H_2O$	0.024	0.024	0.017	-	-0.023	0.008	0.423	0.450	1.983
$CH_3OCHO+OH=CH_3OCO+H_2O$	-0.030	-0.038	-0.015	-	0.067	0.142	-0.361	-0.392	-1.039
$CH_3OCHO+HO_2=CH_2OCHO+H_2O_2$	0.309	0.411	0.566	0.001	0.720	0.564	-	-	-
$CH_3OCHO+HO_2=CH_3OCO+H_2O_2$	0.224	0.306	0.480	0.001	0.604	0.563	-	-	-
$CH_3OCHO+CH_3=CH_2OCHO+CH_4$	0.120	0.078	-0.015	0.001	0.032	-0.031	-	-	-
$CH_3OCHO+CH_3O_2=CH_2OCHO+CH_3OOH$	0.267	0.335	0.707	-	1.116	0.911	-	-	-
$CH_3OCHO+CH_3O_2=CH_3OCO+CH_3OOH$	0.202	0.256	0.582	-	0.895	0.732	-	-	-
$CH_3OCHO+CH_3O=CH_3OCO+CH_3OH$	-0.050	-0.049	0.174	-	0.617	0.499	-0.005	-0.007	-0.020
$CH_3+CO_2=CH_3OCO$	-0.197	-0.197	0.000	-0.000	0.060	-0.003	-0.328	-0.332	-0.175
$CH_3O+CO=CH_3OCO$	0.197	0.197	-0.000	0.000	-0.060	0.003	0.328	0.331	0.175
$CH_2O+HCO=CH_2OCHO$	0.321	0.312	-0.003	0.000	-0.018	-0.001	1.034	1.048	0.114
$CH_3OCO+CH_3OCHO=CH_3OCHO+CH_2OCHO$	-0.143	-0.116	0.061	-	0.232	0.244	-1.220	-1.305	-2.490
$CH_3+CH_2OCHO=CH_3CH_2OCHO$	-0.269	-0.343	-0.048	-	-0.415	-0.570	-	-	-
$CH_2OCHO+HO_2=HO_2CH_2OCHO$	0.006	0.025	0.016	-	0.391	0.627	-	-	-
$OOCH_2OCHO=HOOCH_2OCO$	0.103	0.142	0.020	-	-0.082	-0.005	0.199	0.271	2.400
$HO_2+HO_2=H_2O_2+O_2$	-0.160	-0.244	-0.423	-	-0.695	-1.113	-	-	-
$H_2O_2+M=OH+OH+M$	0.374	0.498	0.921	0.000	1.059	1.911	-	-	-
$HCO+O_2=HO_2+CO$	-	-	-	-0.000	-	-0.001	0.139	0.153	0.048
$CH_3+CH_3(+M)=C_2H_6(+M)$	-0.345	-0.370	-0.009	-	-0.189	-0.171	-	-	-
$CH_4+O_2=CH_3+HO_2$	-0.082	-0.109	-0.025	-	-0.127	-0.178	-	-	-
$CH_3+HO_2=CH_3O+OH$	0.049	0.075	0.016	-	0.156	0.144	-	-	-
$CH_3O_2+HO_2=CH_3OOH+O_2$	0.006	0.014	0.097	-	0.225	0.282	-	-	-
$CH_3O_2+CH_2O=CH_3OOH+HCO$	0.011	0.024	0.090	-	0.289	0.872	-	-	-
$CH_3O_2+CH_3=CH_3O+CH_3O$	0.215	0.235	-0.365	-	-0.562	-0.646	-	-	-
$CH_3O_2+CH_3O_2=CH_3O+CH_3O+O_2$	0.001	0.001	-0.109	-	-0.035	-0.061	-	-	-
$CH_3O_2+CH_3O_2=CH_3OH+CH_2O+O_2$	0.000	-0.001	-0.063	-	-0.060	-0.119	-	-	-
$CH_3OOH=CH_3O+OH$	0.008	0.011	0.087	-	0.174	0.249	-	-	-
$CH_2O+H(+M)=CH_3O(+M)$	0.014	0.014	-0.029	-	-0.153	-0.243	0.001	0.001	0.006
$CH_2O+HO_2=HCO+H_2O_2$	0.019	0.039	0.048	-	0.163	0.558	-	-	-
$NO+OH(+M)=HONO(+M)$	-	-	-	-	-	-	0.017	0.018	0.187
$NO_2+NO_2=NO+NO+O_2$	-	-	-	-	-	-	-0.073	-0.088	-0.414
$CH_2O+NO_2=HONO+HCO$	-	-	-	-	-	-	0.211	0.243	1.004
$HCO+NO_2=NO+CO_2+H$	-	-	-	-	-	-	-0.303	-0.274	-0.035
$CH_3+NO_2=CH_3O+NO$	-	-	-	-	-	-	0.884	0.914	0.596
$CH_3OH+NO_2=HONO+CH_2OH$	-	-	-	-	-	-	0.303	0.330	0.581
$CH_3NO_2(+M)=CH_3+NO_2(+M)$	-	-	-	-	-	-	-0.618	-0.642	-0.522

Figure captions

Fig. 1. High-pressure gas-phase installation.

Fig. 2. Influence of stoichiometry on the MF, CO_2, CO, CH_4, CH_2O and H_2 concentration profiles as a function of temperature in the absence of NO. Sets 1-3 (20 bar) in Table 1.

Fig. 3. Reaction path diagram for MF oxidation in the absence of NO according to the current kinetic model. Solid lines represent the main reaction pathways for all the conditions considered in the present work. The dashed lines refer to additional paths that occur under oxidizing conditions.

Fig. 4. Influence of pressure on the MF, CO_2, CO, CH_4, CH_2O and H_2 concentration profiles as a function of temperature in the absence of NO. Sets 2 and 4-6 (λ=1) in Table 1.

Fig. 5. Influence of the presence of NO on the MF, CO_2 and CO concentration profiles as a function of temperature for different values of lambda. Influence of the stoichiometry on the NO concentration profile as a function of temperature. Sets 7-9 (20 bar) in Table 1.

Fig. 6. Reaction path diagram for MF oxidation in the presence of NO according to the current kinetic model. Solid lines represent the main reaction pathways for all the conditions considered in the present work. The dashed lines refer to additional paths that occur exclusively under oxidizing conditions.

Figures

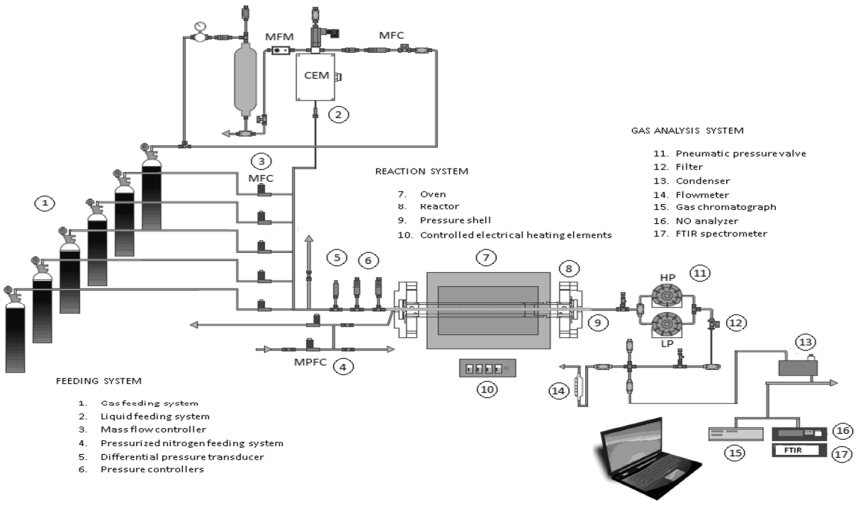

Fig. 1. High-pressure gas-phase installation.

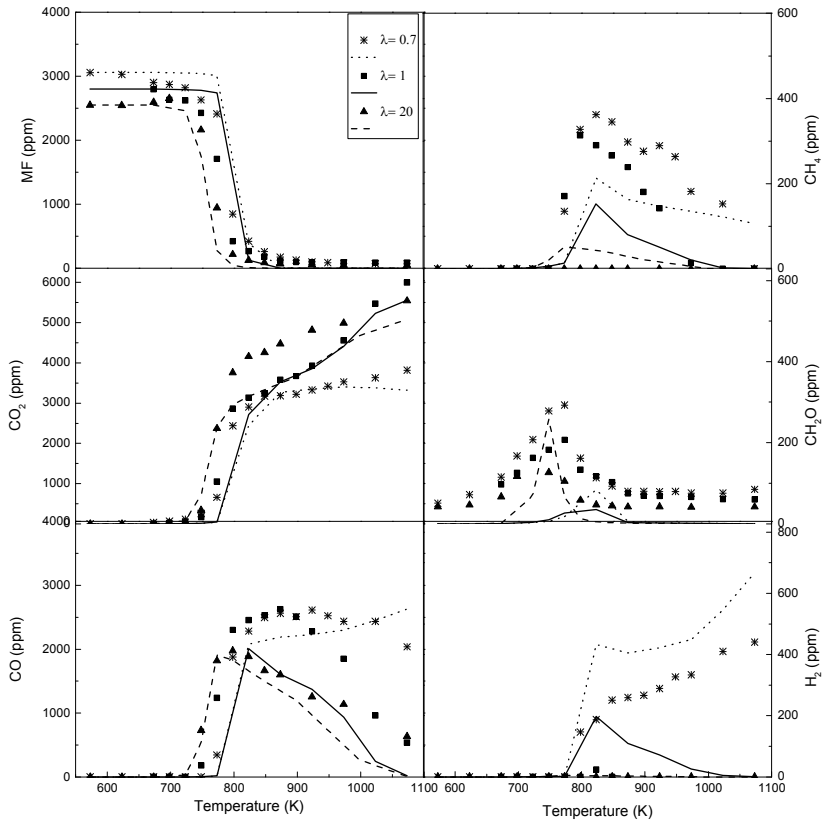

Fig. 2. Influence of stoichiometry on the MF, CO_2, CO, CH_4, CH_2O and H_2 concentration profiles as a function of temperature in the absence of NO. Sets 1-3 (20 bar) in Table 1.

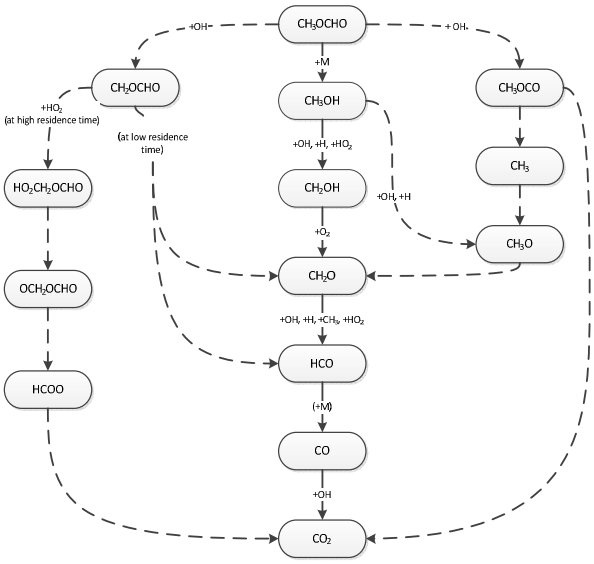

Fig. 3. Reaction path diagram for MF oxidation in the absence of NO according to the current kinetic model. Solid lines represent the main reaction pathways for all the conditions considered in the present work. The dashed lines refer to additional paths that occur under oxidizing conditions.

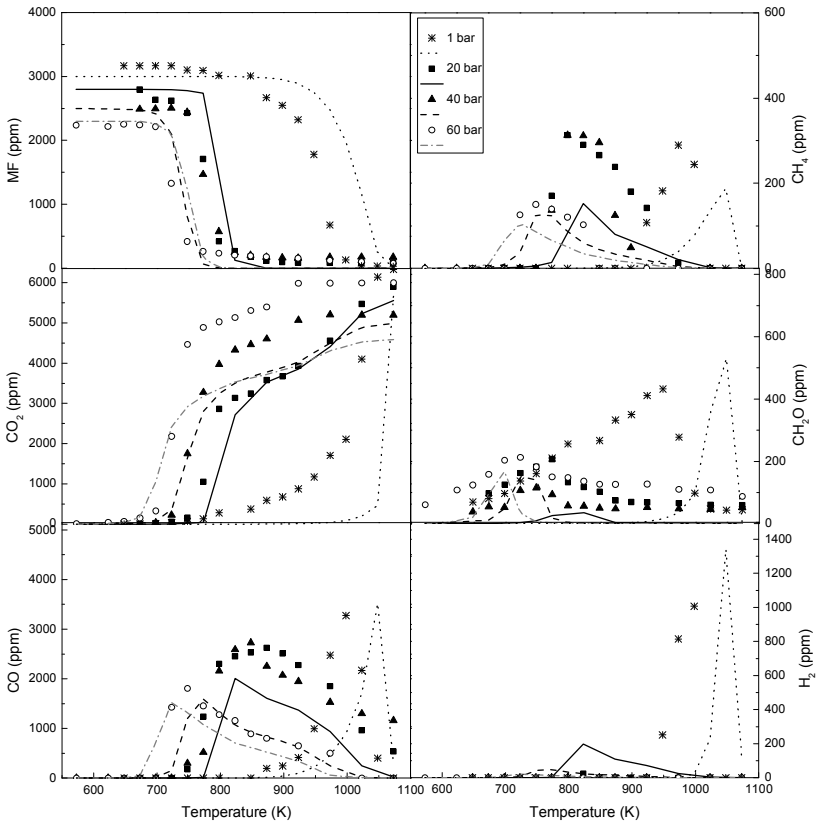

Fig. 4. Influence of pressure on the MF, CO_2, CO, CH_4, CH_2O and H_2 concentration profiles as a function of temperature in the absence of NO. Sets 2 and 4-6 (λ=1) in Table 1.

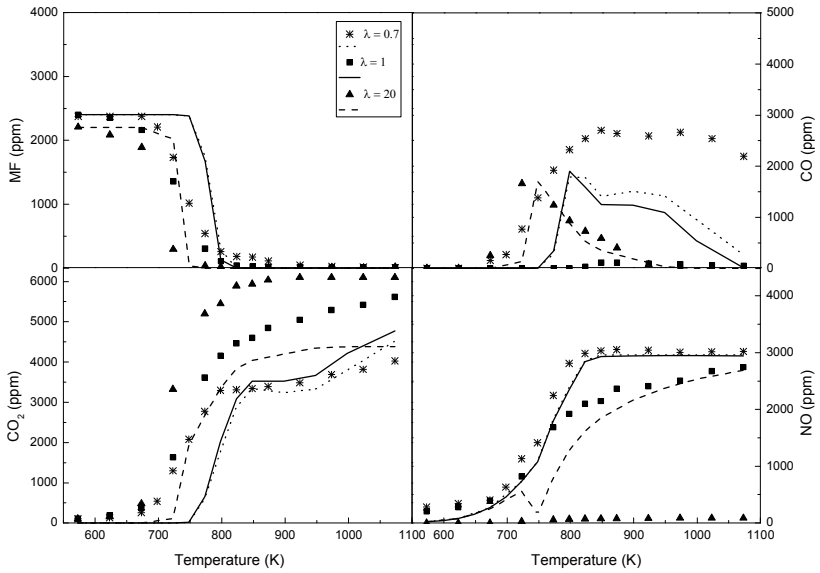

Fig. 5. Influence of the presence of NO on the MF, CO_2 and CO concentration profiles as a function of temperature for different values of lambda. Influence of the stoichiometry on the NO concentration profile as a function of temperature. Sets 7-9 (20 bar) in Table 1.

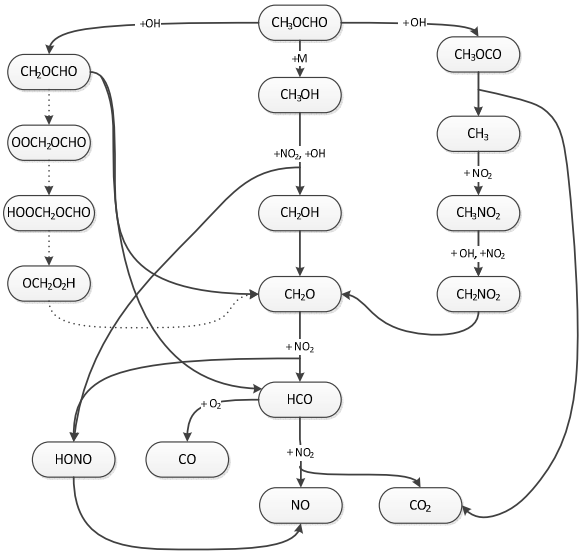

Fig. 6. Reaction path diagram for MF oxidation in the presence of NO according to the current kinetic model. Solid lines represent the main reaction pathways for all the conditions considered in the present work. The dashed lines refer to additional paths that occur under exclusively oxidizing conditions.